

A three dimensional time-dependent approach to calibrating sediment trap fluxes

Ken O. Buesseler,¹ Anthony F. Michaels,² David A. Siegel,³ and Anthony H. Knap²

Abstract. We conducted an experiment to test explicitly the accuracy of upper ocean sediment trap fluxes using the particle-reactive radionuclide ^{234}Th ($t_{1/2}=24.1$ days). Two independent VERTEX-style multitraps were used for collection of sinking particles at 95 m and 97 m depths over a four-day period in May 1992 at the U.S. Joint Global Ocean Flux Study Bermuda Atlantic Time-series Study (BATS) site. Samples for total ^{234}Th were collected every 8 m between the surface and 96 m and immediately combined for analysis to obtain the vertically integrated activity of ^{234}Th . We collected a total of 27 samples over the four-day period. The ^{234}Th samples were collected daily at each of the two traps and every other day on a 6 x 6 km grid to characterize the entire source region for particles collected in the traps. In situ flow sensors at one trap array indicated low horizontal shear at the trap mouth (5-10 cm/s) compared to normal values at BATS. The predicted ^{234}Th flux from the watercolumn profiles was not significantly different from zero (-30 ± 140 disintegrations per minute/m²/d). The measured trap ^{234}Th flux at both arrays was significantly higher (290 ± 15 dpm/m²/d). We hypothesize that upper ocean traps at Bermuda may overcollect during low-flux periods and undercollect during high-flux periods, thus recording a biased signal of the true particle flux.

Introduction

The transport of biogenic and nonbiogenic elements between the surface and deep ocean is thought to be mediated by a range of sinking particulate types. Some of the evidence in support of a rapid settling flux is indirect, such as the presence of fallout artificial radionuclides on the deep seafloor only weeks to months after the early bomb tests [Osterberg *et al.*, 1963]. By far, however, the bulk of our information on sinking particles is collected directly using sediment traps. Traps not only serve as field collectors of material for chemical analyses, but also the interpretation of flux patterns with depth, space, and time has been used to further our understanding of the rates of cycling and remineralization of numerous biogenic and nonbiogenic elements in the oceans (see Fowler and Knauer [1986] for overview). For example, sediment traps have been used to demonstrate how the seasonal pattern of surface productivity is reflected in an increase in organic matter flux to the seafloor during high-productivity events [e.g., Deuser, 1986; Karl *et al.*, 1991; Lohrenz *et al.*, 1992]. Over annual timescales, the input of allochthonous nutrients to surface waters (i.e., new production) is thought to be balanced by export fluxes measured with shallow traps [Eppley and Petersen, 1979; Eppley *et al.*,

1983; Knauer *et al.*, 1990]. Similarly, the measured rates of sinking particulate export are used to explain the distribution and calculate the residence time of a wide range of trace elements in oceanic waters [Livingston and Anderson, 1983; Martin and Knauer, 1984; Buat-Ménard *et al.*, 1989; Buesseler *et al.*, 1990].

Since the advent of sediment traps there have been a variety of studies to evaluate which trap designs and under what field conditions traps can be used as unbiased collectors of sinking particles in the oceans. These studies have focused primarily on hydrodynamic concerns, artifacts related to the collection of nonsinking material ("swimmers"), and the preservation of the sample in the trap. The U.S. Joint Global Ocean Flux Study (JGOFS) sponsored a workshop prior to the first JGOFS field study to address many of these issues, and a major recommendation of this group was to look for independent tests of trapping efficiency, that is, methods to "calibrate" sediment traps [Knauer and Asper, 1989].

The naturally occurring isotopes of thorium have been recommended for use in trap calibration studies on account of their well-known source and decay rates and their simple chemistry and nonselective particle reactivity [Knauer and Asper, 1989]. Measurement of the thorium activity in the oceans can provide an estimate of the particle flux rate, as sinking particles provide the only mechanism other than decay for removing thorium from a given parcel of water. By selecting the thorium isotope with the most appropriate half-life, particle fluxes can be estimated for both surface and deep waters. Thorium-234 ($t_{1/2} = 24.1$ days) is produced at a constant rate from its conservative parent ^{238}U and is most suited to studies of particle export on timescales of days to weeks from surface waters [Buesseler, 1991]. Thorium-230 ($t_{1/2} = 75,000$ years), which is produced from ^{234}U , has been used in studies of deepwater trapping efficiency where residence times are longer [Bacon *et al.*, 1985].

¹Woods Hole Oceanographic Institution, Woods Hole, Massachusetts.

²Bermuda Biological Station for Research, Inc., Ferry Reach, Bermuda.

³Center for Remote Sensing and Environmental Optics and Department of Geography, University of California, Santa Barbara.

The use of ^{234}Th for trap calibration purposes began with Moore *et al.* [1981] who found that measured ^{234}Th trap fluxes from the Santa Barbara basin were 130% of the predicted fluxes. Unfortunately, they did not have ^{234}Th watercolumn and trap data from the same station and depths, so the analyses were quite limited. For many years the best open ocean data for comparing ^{234}Th trap fluxes and those predicted from ^{234}Th watercolumn data were found by Coale and Bruland [1985, 1987]. These researchers examined samples collected during the VERTEX program, perhaps the most ambitious upper ocean trapping program to date. They generally found a good agreement between measured trap ^{234}Th fluxes and those predicted from the watercolumn data; however, the observed/predicted fluxes still ranged from 40-140%. In these early studies, steady state conditions were assumed in order to solve for the ^{234}Th flux using a single ^{234}Th profile. These data and a wide range of field and laboratory studies, suggested that free-floating cylindrical traps of the VERTEX design (aspect ratio ~7-9) could be used as reliable collectors of upper ocean particle flux [Knauer and Asper, 1989].

A larger disagreement between measured and predicted ^{234}Th fluxes was found in subsequent studies using the same VERTEX-style traps in Funka Bay [Tsunogai *et al.*, 1986], Dabob Bay [Wei and Murray, 1992], and in the North Atlantic [Buesseler *et al.*, 1992a]. Many of these newer studies included time series ^{234}Th data, thus permitting the use of non-steady state models to estimate the particulate ^{234}Th flux. None of these studies was designed specifically to evaluate sediment trap accuracy, and the authors could explain the differences between the trap thorium flux and the predicted flux by other processes. More recently, Buesseler [1991] summarized all previously reported experiments with simultaneous measurement of ^{234}Th scavenging and ^{234}Th collection in sediment traps, as well as studies where data were available to make this calculation. In this analysis, measured trap fluxes and predicted fluxes agreed within a factor of two in only one third of the cases. The over or under collecting "biases" were large and unidirectional within a given study, suggesting that the offset was neither random nor small. This comparison included over 50 estimates of upper ocean trapping efficiency, and little support for the earlier more optimistic conclusions drawn from Coale and Bruland could be made.

From the published ^{234}Th literature we can either conclude that traps are frequently inaccurate or that most ^{234}Th investigations are performed in unique environments where the assumptions used to predict flux from scavenging are inappropriate. Since there are no a priori tests of trapping efficiency in the field, it is easiest to question the calibration technique, that is, the sensitivity and accuracy of the modeled ^{234}Th flux. In this regard, arguments have been made that appropriate spatial or temporal considerations are not accounted for when comparing the modeled fluxes and traps, or that advective and diffusive fluxes have not been properly quantified in the ^{234}Th activity balance. Most of these uncertainties arise from the difficulty in determining the three-dimensional, time-dependent flow fields of the water encountered by the trap and the history of ^{234}Th scavenging in that water. In this paper we present data from a more complete study that addresses many of these issues directly. We have tried to conduct an explicit test of the accuracy of free-drifting VERTEX-style multiple particle

interceptor traps (MultiPITS) during a single deployment. For this purpose we collected information on both the spatial and temporal variations in ^{234}Th activity. We also restrict our comparison to the measured and predicted ^{234}Th flux only. While ^{234}Th has recently been used to estimate particulate organic carbon (POC) and particulate organic nitrogen (PON) fluxes [Buesseler *et al.*, 1992a], the conversion of ^{234}Th particle fluxes estimated from its watercolumn distribution to POC or PON flux adds additional uncertainty to the calibration. Claims that trap-derived organic C fluxes are more "reasonable" than ^{234}Th -derived organic C fluxes [Martin *et al.*, 1993] only cloud the issue of whether or not traps collect an unbiased estimate of sediment flux.

Our trap calibration experiment was designed around the JGOFS Bermuda Atlantic Time-series (BATS) site, primarily on account of logistical ease of sampling within an existing trapping program and the availability of background information on the seasonality of flux, productivity, and physical processes. Our initial assumption was that particle fluxes at this site would be small, so extreme care was taken to ensure that the accuracy of each ^{234}Th measurement could be documented and to improve the ^{234}Th analytical precision from $\pm 5-10\%$ or greater, which is typical of previous studies, to better than $\pm 2\%$. Our approach was to collect multiple watercolumn samples within the particle source region of a pair of 100-m free-drifting traps and to sample frequently in time to tightly constrain the watercolumn ^{234}Th activity balance. In addition, measurements were made of surface drift and the approach and interior velocities at the trap.

Methods

Samples were collected May 4-8, 1992, near the BATS site. Measurements were focused around the deployment of two nearly identical sediment trap arrays (PIT-A and PIT-B). The arrays were deployed near $31^{\circ}45' \text{ N}$, $64^{\circ}10' \text{ W}$ ~1.5 km apart. Each array contained MultiPIT crosses [Knauer *et al.*, 1979] at 95 m and 97 m and a package to monitor trap hydrodynamics [Gust *et al.*, 1992] at 93 m. There was a 5-m section of bungee cord at 10 m, immediately above the subsurface flotation. Surface flotation consisted of a series of floats and a single spar. The spar was equipped with Argos and VHF transmitters and a strobe. The traps were deployed for a period of 4 days between 1700 LT on May 4, 1992, and 1800 LT on May 8, 1992.

We collected profiles for ^{234}Th at each trap array on deployment and recovery and every afternoon during the deployment. On May 4, 6, and 8 we also collected 4-5 profiles at a distance of ~6 km from the traps (Figure 1) in all directions. These profiles were performed as quickly as possible; however, with ship repositioning, the traps inevitably drifted a few kilometers from the center of the grid. On both May 5 and 7 we collected two profiles at a distance of 10-12 km from the traps. The locations of these profiles were determined from the drift patterns of the surface drifters (see below) on the previous day, and we attempted to sample "upstream" and "downstream" of the net surface flow by the approximate travel distance of the surface waters in a single day.

Thorium Analyses

We measured the total ^{234}Th activity between the surface and 96 m as a single vertically integrated sample for each station.

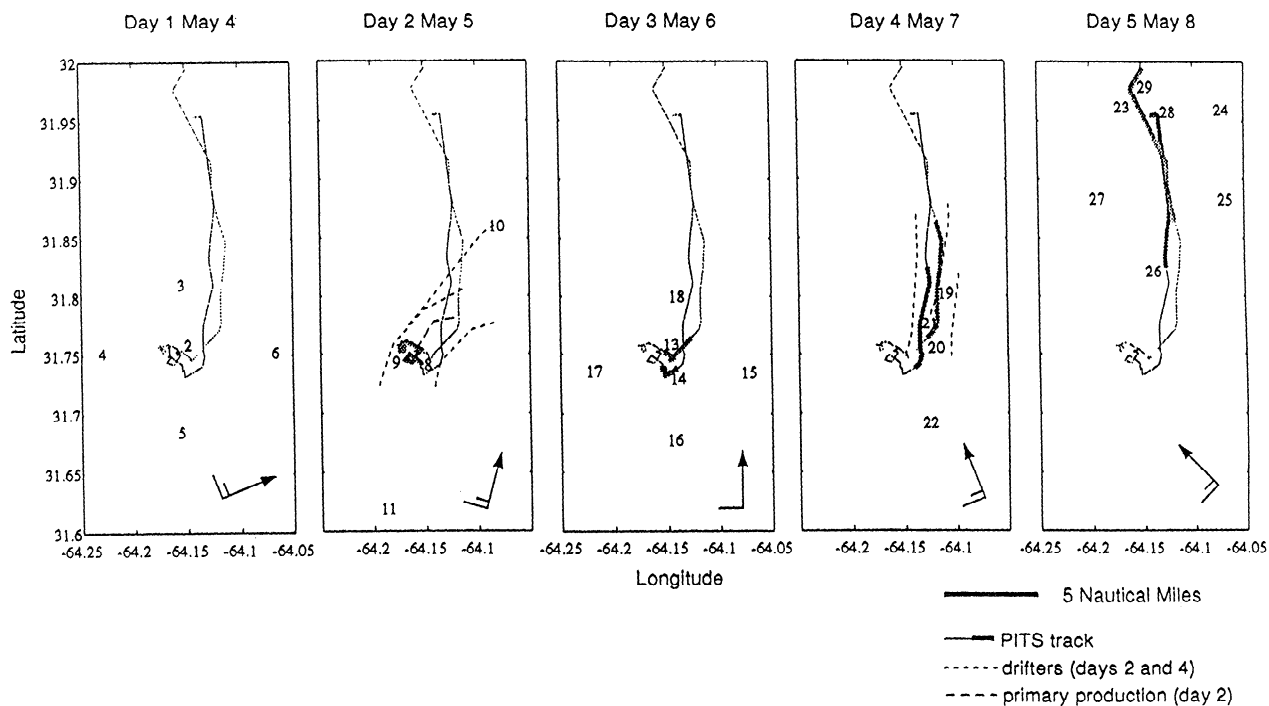


Figure 1. Drifter tracks for the trap calibration experiment in May 1992. The numbers represent the location of the ^{234}Th casts done on each day. The entire drift path of the two trap arrays is shown in each panel, the portion of the drift track actually traveled on that day is the bold portion of the line. The drift tracks of the primary production array and sets of surface drogues are also shown on the appropriate days. The wind arrow in the lower right corner indicates the daily mean wind speed and direction.

This was obtained by collecting water at 12 evenly spaced depths in the upper 96 m (every 8 m between 4 m and 92 m inclusive) with a 12-place rosette containing 12-L Niskin bottles. From each depth we drew a 2-L sample into calibrated, clean polycarbonate bottles. The accuracy of this volume measurement was $\pm 0.3\%$. The 12 2-L samples were dispensed into a 25-L poly-ethylene collapsible container (cubittainer) and mixed well. To each cubittainer we added 1 mL of a 6 disintegrations per minute (dpm)/mL ^{230}Th standard as a yield monitor, 5 mL of FeCl_2 in HCl (50 mg/mL) and 30 mL concentrated HNO_3 . The cubittainers were allowed to equilibrate for 24-60 hours on the ship and were returned to the Bermuda Biological Station for Research (BBSR) within 60 hours of collection for further processing.

At BBSR, each sample was weighed and concentrated NH_4OH was added in order to adjust to $\text{pH}=8$. The Fe precipitate which forms serves as the carrier phase for removing Th (and other radionuclides) from solution. After two settling and centrifugation steps to remove the Fe precipitate from solution, the sample was dissolved in concentrated HCl and treated to ion exchange purification procedures to separate ^{234}Th from other beta emitters [Fleer, 1991; Buesseler et al., 1992b]. The sample was initially passed through an ion exchange column in 8 N HCl (10 mL volume, BioRad AG1x8 100-200 mesh resin). This first column was completed within 3-5 days after sample collection and serves to separate the ^{234}Th from its parent, ^{238}U . A second ion exchange column (5 mL, AG1x8 resin 100-200 mesh in 8 N HNO_3 form) was used for further purification of Th from other potential beta emitters. The final

purified Th fraction was taken to dryness in a 100-mL beaker and mailed to Woods Hole Oceanographic Institution (WHOI) Woods Hole, Massachusetts, for plating and low-level beta counting.

At WHOI, each sample was redissolved and electroplated onto a stainless steel planchette. Samples were first alpha counted for 24 hours for ^{230}Th to obtain the overall chemical yield. Subsequently, the planchettes were mounted with a 9 mg/cm^2 foil cover (to reduce any low-energy beta emissions) and counted on gas flow proportional counters. The beta detectors have an average background count rate of 0.4-0.5 cpm [Noshkin and DeAgazio, 1966]. Blanks were run to ensure that there was no ^{234}Th beta activity associated with our yield monitor or reagents. The ^{234}Th activity was quantified by detecting the much stronger beta signal of its immediate daughter, ^{234}Pa (Energy = 2.3 MeV; $t_{1/2} = 1.2$ min). The detection efficiency for the $^{234}\text{Th}/^{234}\text{Pa}$ pair is $\sim 50\%$ and was determined separately for each of the 12 beta counters. Ultimately, the ^{238}U /salinity relationship of Chen et al. [1986] (3.238 nano gram ^{238}U per g seawater at 35.0‰) and four deepwater samples were used to finalize the calibration of each detector (see Results).

To improve precision and accuracy, each sample was counted 5-6 times on the same detector for three 500-min cycles over a period of 50-60 days. We then used a curve fitting routine (Sigma Plot Scientific Graph System) to fit the 15-18 separate beta determinations in order to calculate the net ^{234}Th activity and associated error at t_0 and the total background activity. The advantages of this approach over a single ^{234}Th beta

determination are that (1) precision is increased, as multiple determinations of the counting activity reduce the statistical error on the total t_0 activity; (2) fluctuations in the background count rate are averaged in the calculated background activity, thus improving confidence in the accuracy of the net beta activity determination (= total activity at t_0 - background cpm); and (3) since the beta signal is fit to a 24.1-day half-life decay rate, this ensures that any non ^{234}Th -derived beta activity is not included in the calculated net ^{234}Th signal, as some short-lived beta emitters are easily picked up during plating. The ^{234}Th activity was also corrected for ingrowth from ^{238}U between sampling and our first ion exchange column.

If we had only beta counted each sample a single time, as is more commonly done, then there would be no way of ensuring that the true ^{234}Th activity was within the one sigma counting uncertainty of any single determination. We found that the difference between ^{234}Th activity determined from the first beta count and ^{234}Th determined from our curve-fitting technique could be as large as 6%, which is unacceptable for our purposes. Furthermore, given our small beta counting errors (± 1 -2%), we found that the uncertainty on the determination of our yield monitor was significant (initially >2%). Therefore we recounted every sample for ^{230}Th on the alpha detectors an additional 48-72 hours in order to reduce the error on the yield determination to <1% (see discussion of deepwater replicates).

Trap Fluxes

The sediment traps were standard VERTEX-style MultiPITS [Knauer *et al.*, 1979, 1990; Martin *et al.* 1987] and are described in detail in the BATS Methods Manual [Knap *et al.*, 1993]. Briefly, each sediment trap tube is a polycarbonate cylinder with a cross-sectional area of 0.0039 m². The upper 8 cm of the tube is equipped with a removable baffle constructed of 14 pieces of 1.2-cm ID polycarbonate pipe. The trap tubes are mounted on a polyvinyl chloride (PVC) cross attached to the array at the appropriate depths. The sediment traps are filled with a 50 parts per thousand (ppt) brine solution which contains 2% formalin prior to deployment. The upper part of this brine solution is removed by the flow of water through the trap during the deployment to a characteristic depth in the trap tube. This brine-seawater interface is readily apparent through the transparent tubes. Upon recovery, the solution above the interface is removed.

We used two trap tubes on each array to make carbon and nitrogen flux estimates. After recovery, the trap tubes were drained through the filtration frit and a 90-mm polycarbonate filter was mounted on the bottom of the trap by gravity. All of the visible swimmers were removed from this filter with very fine forceps under 25x magnification on a high-quality dissecting microscope. For a 150-m trap from BATS, this manual swimmer removal typically takes from 2-6 hours for each trap tube. Swimmers as small as 300 μm are removed effectively (though not completely), and swimmers as small as 100 μm are partially removed. There are cryptic swimmers and swimmer products that cannot be removed at all [Michaels *et al.*, 1990]. The use of the smooth membrane filters greatly enhances the ability to remove zooplankton. Such removal is much more difficult and less complete when the material is collected on glass fiber filters. We have estimated that even with these extensive efforts to remove the zooplankton, 10-40%

of the carbon that remains in the trap is probably swimmer or swimmer-related material [Lohrenz *et al.*, 1992]. After picking the sediment traps, the remaining material was dried and weighed, and aliquots were measured for carbon and nitrogen content. Carbon was also measured on acidified and nonacidified aliquots to estimate the carbonate flux by difference. For this paper we use the organic carbon and nitrogen fluxes only.

We deployed eight trap tubes for thorium fluxes at each depth (95 and 97 m) on each trap array, thus obtaining four ^{234}Th trap samples (PIT-A 95 m, PIT-A 97 m, PIT-B 95 m, PIT-B 97 m). The larger number of trap tubes increases the thorium signal. This improves the precision of the flux estimate and allowed us adequate material to resolve signals on the swimmer fractions of the material. The eight trap tubes from a single array and depth were combined onto one 47-mm Whatman GF/F filter by pouring the contents into a filter funnel under low vacuum. We then rinsed all trap tubes with dilute HCl (1 N) to remove adsorbed thorium or any particles that were caught up in the baffles or were stuck to the sides and bottom. The combined trap wash solution from all thorium trap tubes ($n = 32$) was analyzed as a single sample. The filters were then examined under a dissecting microscope and the swimmers removed as above. Swimmer removal on GF/F filters is less complete than on membrane filters, so we measured the thorium activity on the swimmer fractions to estimate the possible size of a swimmer artifact. We also separated the swimmers into two size groups. Large swimmers (generally, the obvious crustacea larger than 1000 μm length) were removed first. These zooplankton are typically removed completely by most investigators who actually try to remove swimmers manually. Small swimmers were removed later under 25x magnification. Small swimmers (smaller crustacea and noncrustacean swimmers) are only effectively removed by the methods and effort described above. We estimate that we removed between 60-90% of the small swimmers that were removed from the carbon flux traps. Because of the relatively small amount of thorium on these swimmers (see results), we estimate that this residual swimmer bias is small for the thorium flux.

The activity of ^{234}Th on the trap samples was estimated using a slight modification of the techniques for the water samples. In this case, each trap or swimmer sample was digested in warm 8 N HNO₃ for 12-24 hours in the presence of our ^{230}Th yield monitor. Each sample was subsequently passed through a 10-mL AG1x8 column in the 8 N HNO₃ form. After the thorium is eluted with 8 N HCl, the purification steps become identical to those described for the watercolumn samples. All of the ^{234}Th flux data are decay corrected to the midpoint of the trap deployment assuming a constant flux. Analytical errors are based upon counting statistics alone, using a curve fitting procedure identical to the treatment of the watercolumn beta counting results.

Hydrography

To characterize the biogeochemistry of the water, we measured the full set of BATS core parameters in the upper 250 m during the cruise. These measurements included hydrography (conductivity-temperature-depth (CTD) and wet salinity measurements), oxygen, nutrients, particulate organic carbon and nitrogen, phytoplankton pigments by high pressure

liquid chromatography, bacteria abundance, and primary production by ¹⁴C uptake. These measurements were made by the BATS technicians using the standard BATS protocols [Knap *et al.* 1993; Michaels *et al.*, 1994]. We also collected casts with an optical package that contained a spectral radiometer, transmissometer, fluorometer, and CTD. The optics data will be presented elsewhere, however, we used the temperature profiles from nearly 40 casts with the optical package and the 33 casts with the CTD as additional information on the hydrography and to help with the calibration of the flow sensors on the hydrodynamic sensing (HDS) packages on the traps.

Hydrodynamic Sensing Packages

We monitored the flow environment around the sediment traps and the motions of the mooring lines on a trap array A with an HDS package designed and built by Giselher Gust (the HDS package on trap array B failed). The HDS package consists of a set of four small velocity sensors that operate on the hotfilm principle [Blackwelder, 1981]. These sensors measured the speed of the flow parallel to the sensor plane with a threshold value of 0.5 cm/s and an accuracy of better than 3%. Sensors were calibrated both before and after the cruise using a laser doppler velocimeter system. Two of the sensors were placed at either end of the arms of a modified sediment trap frame, and two were placed inside separate sediment trap tubes just below the baffle on the downstream side. This frame was mounted at 93 m and vaned to keep it oriented into the ambient flow. The HDS packages also had sensors to monitor package tilt, temperature, and pressure. Data were collected and stored internally on an ONSET tattletale computer. The HDS package, calibration procedures, and data analysis methods are described in more detail elsewhere [Gust *et al.*, 1992; also unpublished data, 1994].

Drifters

We deployed three surface drifters for periods of 12 hours on both May 5 and 7, 1992. These drifters consisted of a 1-m diameter sea anchor, held open with a PVC cross suspended from a small surface spar by 5 m of 1/4-inch nylon line. The spars were made of 1-inch aluminum pipe with a 10-kg weight at one end, ~20 kg of flotation in the middle, and a flasher at the other end. The sea anchor was also weighted with a 2.5-kg lead weight. These crude drogues were used to estimate the velocity of the near-surface currents and to estimate horizontal eddy diffusivities using the techniques of Hitchcock *et al.* [1990].

With these surface drifters, a 150-m primary production array, and the two sediment trap arrays of 120 m total length, we had as many as six drifters in the water at one time. Each drifter was visited as frequently as possible, and Global Positioning System positions were recorded.

Results

Hydrography and Biogeochemistry

May is a period of transition from the deeper winter mixed layers, which typically lead to elevated surface nutrients and high primary production rate, and the highly stratified conditions in the summer. During this cruise there were relatively shallow mixed layers of 30-60 m with weak thermal stratification near the surface, particularly at the end of the cruise, and between the surface mixed layers at 21°C and the 18°C mode water at 300-400 m depths. Internal wave activity resulted in fluctuations of the mixed layer and thermocline of up to 30 m with a period of ~24 hours. Nutrient profiles showed a surface depletion with the top of the nitricline at 120 m. There was a strong subsurface chlorophyll maximum layer at 125 m that exhibited both the internal wave variability and a strong diurnal pattern in the mixed layer. The integrated primary production rate was 616 mg C/m²/d, with measurable production at 120 m. This is very different from the production rates and profiles for the preceding months and next few months which showed strong surface maxima in production and no production below 100 m.

Watercolumn ²³⁴Th

Since the absolute ²³⁴Th activity is critical to any ²³⁴Th particle flux estimate, we analyzed four deepwater samples collected from 900 m on a single CTD/Rosette cast to ensure overall accuracy of our detector calibration and to determine the precision of our analysis. In deep waters, ²³⁸U and ²³⁴Th activities are known to be in secular equilibrium, as particle fluxes are negligible relative to total production and decay rates [Coale and Bruland, 1985; Buesseler *et al.*, 1992a]. The reliability of the ²³⁸U estimate is not generally in question, since Chen *et al.* [1986] show a constant ²³⁸U/salinity relationship in the Atlantic and Pacific to within a standard deviation of 0.7% (n=21). We confirmed this relationship at BATS by measuring ²³⁸U directly at 110 m and 900 m using thermal ionization mass spectrometry, and found agreement within 0.1% relative to Chen *et al.* [1986] (R. L. Edwards, unpublished data). Given a salinity of 35.254‰ for our deepwater sample, we calculated an

Table 1. Deepwater Samples

	Depth, m	Collection Date, dd/mm/yr	Salinity, ppt	²³⁴ Th, dpm/kg	±Error, %	²³⁴ Th, dpm/kg	
						Mcan ± s.d.	Calculated ^a
1	900	April 24, 1992	35.254	2.37	1.4	2.425 ± 0.049	2.418
2	900	April 24, 1992	35.254	2.45	2.2		
3	900	April 24, 1992	35.254	2.40	1.4		
4	900	April 24, 1992	35.254	2.48	2.0		

^a ²³⁴Th calculated from secular equilibrium with uranium (=0.0686 × salinity) [Chen *et al.*, 1986].

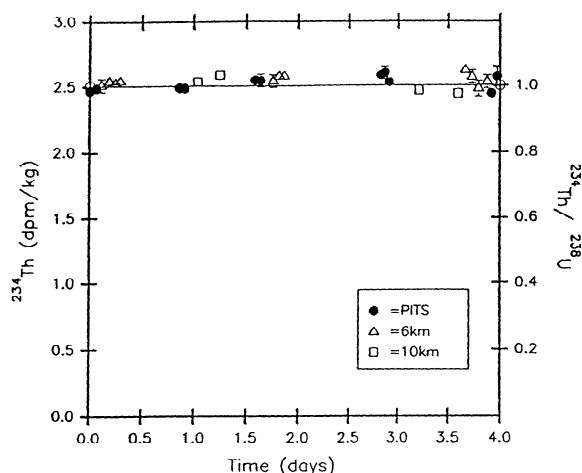


Figure 2. Integrated water column ^{234}Th activities throughout the May 1992 trap calibration experiment. Solid circles are the measurements at the different trap arrays. Open triangles are the measurements made at 6-km distances from the arrays (see Figure 1 for locations). Open squares are measurements made 10 km away from the arrays. The solid line represents the equilibrium ^{234}Th activity throughout the experiment.

expected ^{238}U activity of 2.418 dpm/kg. Treating each sample as an unknown, we determined a mean deepwater ^{234}Th activity of 2.425 ± 0.049 ($n = 4$; Table 1). This is not surprising since we used all of these deepwater samples for our final calibration of each of the 12 beta detectors. A change in the ^{238}U /salinity relationship beyond that found by *Chen et al.* [1986] would only shift the absolute activity of ^{238}U and ^{234}Th , and our observation of secular equilibrium in surface waters at higher salinity (see below) would still hold. Since the total activity deviation between these deepwater replicates ($\pm 2\%$) is the sum of counting errors (average $\pm 1.4\%$) and other undetermined errors (such as weighing errors, ^{230}Th yield determination, spike calibration, etc.), we estimate that the average error on a given sample in addition to beta counting statistics is $\pm 0.9\%$. For each subsequent ^{234}Th activity reported here we therefore report not only the counting error (as is typically done) but also propagate this additional 0.9% uncertainty.

The most striking result was the high and invariant total ^{234}Th activity (Figure 2). The mean ^{234}Th activity for all of the data was 2.53 dpm/kg with a standard deviation of only 0.05 ($n=26$). Individual errors range from ± 1.2 -3.2% and average ± 0.05 dpm/kg (Table 2). Details on spatial and temporal variability in ^{234}Th activity and some further statistical analyses

Table 2. BATS Watercolumn ^{234}Th Activity Data

Sample Description	Salinity	Collection Date	Bermuda Time, LT	Total ^{234}Th , dpm/kg ^a	Error ^b		dpm/m ² /d ^c
					+/-	%	
C1: 0-96m @PIT-B	36.766	May 4, 1992	1715	2.47	0.03	1.3	152.8
C2: 0-96m @PIT-A	36.766	May 4, 1992	1845	2.49	0.03	1.3	101.4
C3: 0-96m 6 km N	36.737	May 4, 1992	1955	2.51	0.05	1.9	28.9
C4: 0-96m 6 km W	36.732	May 4, 1992	2145	2.54	0.03	1.2	-64.0
C5: 0-96m 6 km S	36.788	May 4, 1992	2305	2.53	0.03	1.3	-9.0
C6: 0-96m 6 km E	36.792	May 5, 1992	0015	2.54	0.03	1.2	-52.4
C8: 0-96m @PIT-A	36.776	May 5, 1992	1355	2.49	0.03	1.4	100.4
C9: 0-96m @PIT-B	36.777	May 5, 1992	1500	2.49	0.03	1.4	104.9
C10: 0-96m 10 km downstream	36.773	May 5, 1992	1810	2.54	0.03	1.2	-47.4
C11: 0-96m 10 km upstream	36.797	May 5, 1992	2315	2.59	0.04	1.5	-190.8
C13: 0-96m @PIT-B	36.782	May 6, 1992	0715	2.55	0.04	1.7	-77.5
C14: 0-96m @PIT-A	36.786	May 6, 1992	0830	2.54	0.05	2.0	-63.2
C15: 0-96m 6 km E	36.785	May 6, 1992	0945	2.82	0.06	2.3 ^d	-883.5
C16: 0-96m 6 km S	36.789	May 6, 1992	1125	2.54	0.05	1.8	-49.5
C17: 0-96m 6 km W	36.770	May 6, 1992	1250	2.58	0.03	1.3	-169.5
C18: 0-96m 6 km N	36.773	May 6, 1992	1400	2.58	0.04	1.5	-171.0
C19: 0-96m @PIT-B	36.785	May 7, 1992	1300	2.58	0.04	1.7	-181.4
C20: 0-96m @PIT-A	36.788	May 7, 1992	1400	2.60	0.05	1.8	-227.3
C21: 0-96m @PIT-A	36.788	May 7, 1992	1500	2.53	0.03	1.4	-21.9
C22: 0-96m 10 km upstream	36.793	May 7, 1992	2220	2.47	0.04	1.5	172.5
C23: 0-96m 10 km downstream	36.757	May 8, 1992	0730	2.44	0.04	1.6	231.6
C24: 0-96m 6 km E	36.759	May 8, 1992	0910	2.62	0.03	1.2	-300.8
C25: 0-96m 6 km S	36.788	May 8, 1992	1045	2.57	0.05	2.0	-140.3
C26: 0-96m 6 km W	36.796	May 8, 1992	1215	2.48	0.06	2.5	129.0
C27: 0-96m 6 km N	36.729	May 8, 1992	1415	2.53	0.05	1.9	-38.7
C28: 0-96m @PIT-A	36.754	May 8, 1992	1515	2.45	0.04	1.7	225.6
C29: 0-96m @PIT-B	36.747	May 8, 1992	1635	2.57	0.08	3.2	-150.7

^a Total ^{234}Th activity average between 0-96 m calculated at time of collection.

^b Error propagated from counting statistics (from curve fit to beta data) and other analytical/field errors (+/- 0.9% from deepwater replicates).

^c ^{234}Th flux calculated from steady state model and $^{238}\text{U}=2.52$ dpm/kg (from $^{238}\text{U}=\text{salinity} \times 0.0686$; *Chen et al.*, [1986]).

^d Data from C15 not included in statistical analyses as chemical yield low (<25%) hence elevated ^{234}Th activity.

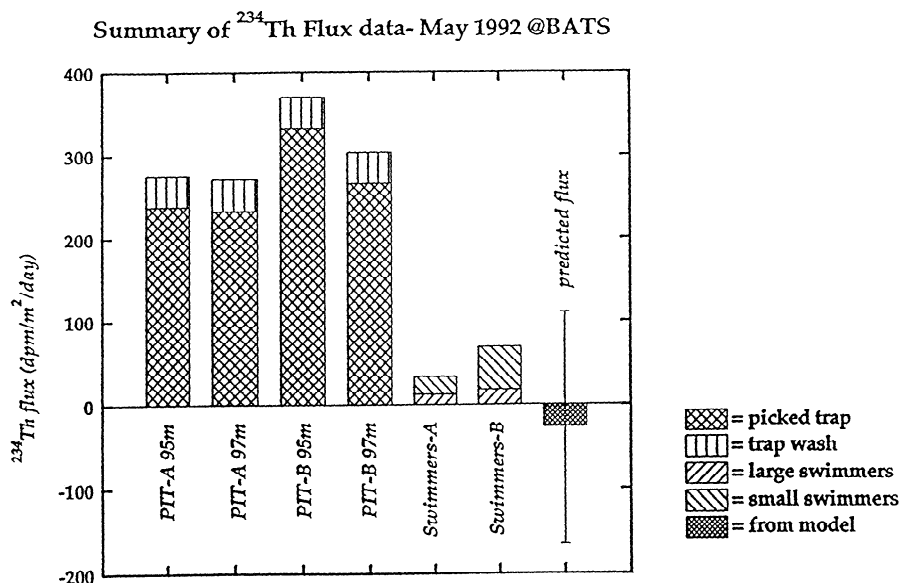


Figure 3. Summary of ^{234}Th flux data from the sediment traps. Large swimmers are those obvious under low magnification (6x) on a dissecting microscope and are generally larger than 800 μm . Small swimmers are those removed by a trained person under high magnification (35-50x). These include zooplankton as small as 100 μm and some of the cryptic zooplankton. Trap wash is from 1 N HCl rinse of trap tubes. Predicted flux with associated uncertainty is from steady state model (see text for details).

of these data will be presented in more detail below, as they pertain to the calculated particulate ^{234}Th fluxes. Uranium-238 activities calculated from salinity are constant within 1% and indicate a parent ^{238}U activity of 2.52 dpm/kg.

Sediment Traps

Thorium fluxes in the four traps range from 233-333 dpm/m²/d, depending upon the removal treatment for swimmers (Figure 3 and Table 3). The traps at 97 m were handpicked to exclude both large and small swimmers (see Trap Fluxes). An average ^{234}Th flux of 290 dpm/m²/d was found at 97 m, with a slight elevation in trap PIT-B relative to trap PIT-A similar to

mass and POC/PON fluxes (flux A/B = 89%; see Table 4). The swimmer activities were determined by combining material from both 95 and 97 m from a single trap array A or B and are all much lower than the total ^{234}Th flux (5-20% for any fraction; Table 3). The ^{234}Th activities on the small swimmer fraction are 2-3 times higher than the large swimmer fraction (Table 3). The low total swimmer ^{234}Th activities in general are in sharp contrast to organic C and N swimmer corrections for these traps, where the swimmer organic C mass removed from the trap would exceed the total passive C flux. The much lower swimmer ^{234}Th flux relative to C is thought to be due to the lower surface to volume ratio of the large swimmers, resulting in

Table 3. Sediment Trap ^{234}Th Flux

	Depth, m	^{234}Th Flux, dpm/m ² /d		Swimmer Flux, dpm/m ² /d		Wash, dpm/m ² /d ^e	Net ^{234}Th Flux, dpm/m ² /d ^f
		Without Any ^a	Without Large ^b	Large ^c	Small ^d		
PIT-A	95	—	238 (2%)	12 (8%)	22 (14%)	38 (3%)	—
PIT-A	97	233 (3%)	—	12 (8%)	22 (14%)	38 (3%)	271 (3%)
PIT-B	95	—	333 (3%)	18 (6%)	51 (10%)	38 (3%)	—
PIT-B	97	266 (3%)	—	18 (6%)	51 (10%)	38 (3%)	304 (3%)

Values in parentheses indicate analytical uncertainty.

^a ^{234}Th flux for trap picked for both small and large swimmers (see text for details).

^b ^{234}Th flux for trap picked for large swimmers only.

^c ^{234}Th flux measured on large swimmer fraction (95 and 97-m samples combined).

^d ^{234}Th flux measured on small swimmer fraction (95 and 97-m samples combined).

^e Wash flux represents ^{234}Th on particles and solution adhering to trap walls (see text).

^f Net ^{234}Th flux is sum of wash (column 7) and completely picked trap (column 3).

Table 4a. Sediment Trap Flux Data

	Depth m	Mass mg/m ² /d	POC		PON		C/N-Mole
			Milligrams per Square Meter per Day	Micromoles per Square Meter per Day	Milligrams per Square Meter per Day	Micromoles per Square Meter per Day	
PIT-A	95	81	19	1.6	3.4	0.24	6.6
PIT-A	97	95	24	2.0	4.6	0.32	6.2
PIT-B	95	92	24	2.0	4.6	0.33	6.3
PIT-B	97	105	29	2.4	5.7	0.41	5.8

Table 4b. Sediment Trap Flux Ratios

	PIT-A/PIT-B
Depth, m	97
Mass, %	89
POC, %	81
PON, %	77
²³⁴ Th, %	89

Table 4c. Sediment Trap POC/²³⁴Th and PON/²³⁴Th Ratios

	Depth, m	POC/ ²³⁴ Th, μmol/dpm	PON/ ²³⁴ Th, μmol/dpm
PIT-A	97	6.6	1.0
PIT-B	97	7.3	1.2

lower activities of the surface reactive ²³⁴Th tracer in these larger biological materials.

Of equal magnitude as the swimmer flux but much lower than the total ²³⁴Th flux, was the trap wash (Table 3). The ²³⁴Th activity in this wash was found to be equivalent to a ²³⁴Th flux of 38 dpm/m²/d. In most previous studies, traps are neither picked for swimmers when ²³⁴Th is determined nor rinsed after the trap solution is poured off. As seen here, the magnitude of these corrections is generally small, and the direction of the swimmer and wash corrections to the trap fluxes would be in opposite directions. For example, for PIT-A the combined large and small swimmer flux totals 34 dpm/m²/d which would be a positive bias to the trap flux, and the average wash correction is 38 dpm/m²/d, which would be a negative bias. In PIT-B the swimmer flux is close to twice the wash correction. For purposes of our discussion we have added the wash flux to the completely picked samples from 97 m (a 15% correction), resulting in a mean ²³⁴Th flux of 287 dpm/m²/d for both arrays.

An average mass flux of 88 and 99 mg/m²/d was found for PIT A and B, respectively. POC fluxes averaged 21.5 and 26.5 mg/m²/d, and PON fluxes averaged 3.96 and 5.15 mg/m²/d at PIT A and B, respectively (Table 4). Therefore similar to ²³⁴Th, replicates for mass, POC, and PON flux at 97 m show constantly higher fluxes by ~10-20% in PIT-B relative to PIT-A. C/N ratios average 6.2 (molar ratio) for the trap material (Table 4).

Flow and Drifter Patterns

The sediment trap drift patterns fell into two distinct phases. During the first two days of the deployment, the sediment traps moved very little (Figure 1). They converged slightly from an initial separation of 1.5 km to a separation of 1 km after 40 hours. After ~60 hours there was a rapid divergence of the two traps to a separation of over 4.5 km 95 hours after deployment. During this divergence, the traps also increased

their drift rate to between 15-25 cm/s and moved off to the north and later the northwest. The primary production array was deployed on May 5 with a similar depth distribution of drag and followed a very similar course.

The surface drifters showed a very different movement pattern (Figure 1). Despite the stability of the sediment traps on the first two days, the surface drifters on May 5 moved northeast at a rate ranging from 26 to 30 cm/s. On May 7 these same drifters moved due north at 16-28 cm/s. The difference in the drift rates of surface water and the sediment traps with their additional drag at deeper depths indicates that there may have been substantial shear in the watercolumn at some depths to either balance the surface flows in the early part of the trap deployment or to modify the course in the later part.

The flow sensors on the PIT-A array indicated that flows around these traps were relatively low during this deployment (Figure 4). The mean approach velocity was 8.2 cm/s, averaged over the entire deployment. Internal downwelling velocities averaged 1.2 cm/s. Velocities were relatively consistent throughout the deployment with a 5-hour burst of higher velocities beginning at hour 90. There was good coherence between all of the probes. Package tilt was generally less than 6° (Figure 4). The hourly averaged data from the pressure sensor indicated that vertical movement of the trap was confined to about a 1-m depth change, however, the higher frequency data (sampled at 5 Hz) showed rapid vertical excursions of 0.7 m in 3 s. Analyses of the spectra of the pressure and flow sensor data showed distinct peaks at periods of 8-15 s, indicating that surface waves were influencing the movement of the trap array.

Discussion

Trap Calibration

In our experiment we measure ²³⁴Th trap fluxes and compare them to the calculated ²³⁴Th particle flux which is necessary to

maintain the observed watercolumn activity balance. To make this comparison, we sampled at 27 points in space and time in the vicinity of the two trap arrays. To a first approximation, all of the total watercolumn thorium activities are the same, as reflected in the narrow standard deviation in the activity of these samples

($\pm 2\%$; Table 2). There does, however, appear to be more scatter in the ^{234}Th activities near the end of the experiment (Figure 2), perhaps as a result of the increased drift during the second half of the experiment (Figure 1) and, potentially, the sampling of water masses with different scavenging histories.

To determine if there is any significant spatial or temporal trend in the data, we performed an analysis-of-covariance test with one factor (sample location, i.e., @PITS or @6km) and one covariate (time). Using a randomization procedure that reassigns the observed data within this study to a different sample location or time factor, we can find no statistically significant spatial or temporal trend in the ^{234}Th watercolumn data (p value = 0.344). In examining the data in this fashion, we are assuming that the trap is collecting particles from a given parcel of water over the 4-day period. As such, temporal changes in ^{234}Th activity would be driven by seasonal or at least regional changes in biological activity (i.e., scavenging intensity), and any horizontal activity gradients must be maintained by fixed particle source or sink regions. At BATS, given the relatively small particle source region for a 100-m floating trap (1-6 km, see following discussion in Particle Source Region) and the relatively high surface currents (10-20 km/d), our traps may more aptly be considered as "fixed" collectors of sinking particles from numerous parcels of water which pass over the trap for a short period, each characterized by its own ^{234}Th activity balance and sinking particle flux (i.e., a Lagrangian approach). Prior to the thorium flux modeling, we will address this issue of the particle source region or "statistical funnel" for traps [Deuser *et al.*, 1988; Siegel *et al.*, 1990; Hitchcock *et al.*, 1990].

Particle Source Region

To estimate the effective area from which our traps are collecting particles, we use two approaches. First, we use a procedure similar to Hitchcock *et al.* [1990]. For this analysis, the eddy diffusivity is calculated from the "neighbor diffusivity," $F(\ell)$ (in cm^2/s), based upon the relative difference between our surface drifters. Values for $F(\ell)$ are determined from the equation:

$$F(\ell) = (\ell_1 - \ell_0)^2 [2t]^{-1} \quad (1)$$

where ℓ_0 and ℓ_1 are successive separation distances for each buoy pair at time intervals of t (seconds). Using this approach and our surface drifter data (Figure 1), we calculate a surface horizontal diffusivity of 0.5×10^4 and $3.3 \times 10^4 \text{ cm}^2/\text{s}$ for drifter experiments 1 and 2, respectively. This diffusivity is used to calculate a corresponding length scale for point source dispersion, using a relationship determined empirically from dye release experiments [Okubo, 1971], namely:

$$K_h = 0.0103L^{1.15} \quad (2)$$

where K_h is the diffusivity (cm^2/s) and L is the length scale (cm) of interest. Using our diffusivities, we calculate a horizontal

length scale of $<1\text{-}5$ km. Given that a drifting trap moves with the flow to some extent, the actual particle source region should be even smaller.

We can also estimate the sampling length scale L as the horizontal distance that a particle traverses as it sinks through a vertically sheared current. The time required for the particle to reach the trap T is related to its sinking rate w_s and the depth of the trap D or $T = D/w_s$. Similarly, the depth where the particle will be found z_p will be equal to $w_s t$, where t is time from release at the surface. The length scale L can then be calculated as the distance upstream relative to the drifting trap from where the particle originated, or

$$L = \int_0^T \frac{\partial U}{\partial z} z_p dt = \int_0^T \frac{\partial U}{\partial z} w_s t dt = \frac{1}{2} \frac{\partial U}{\partial z} \frac{D^2}{w_s} \quad (3)$$

where $\partial^{234}\text{Th}/\partial t$ is the mean vertical shear of the horizontal current above the trap.

To estimate $\partial U/\partial t$, we can use the difference in velocity measured between the surface drifters and the approach velocity measured at the trap depth with the HDS package (15 cm/s). From this, and using a sinking speed of 100 m/d, we calculate from (3) a length scale $L = 6.3$ km. With a sinking speed of 50 m/d, $L = 12.5$ km. These estimates of the particle source region for our trap indicate a length scale of the order of 1-10 km. As such, we feel that the sampling strategy chosen here, that is, the 6-km grid surrounding the trap, is appropriate for characterizing the ^{234}Th - ^{238}U disequilibria of the particle source region.

^{234}Th Modeling

In surface waters, the ^{234}Th activity is determined by a balance between its production from ^{238}U , radiodecay of ^{234}Th , removal onto rapidly sinking particles, and by supply and loss due to advective and diffusive gradients. Mathematically, the surface water ^{234}Th activity balance can therefore be described by the following equation:

$$\frac{\partial^{234}\text{Th}}{\partial t} = {}^{238}\text{U}\lambda - {}^{234}\text{Th}\lambda - P + V \quad (4)$$

where $\partial^{234}\text{Th}/\partial t$ is the change in ^{234}Th activity with time, ^{238}U is the uranium activity determined from salinity (^{238}U (dpm/kg) = $0.0686 \times \text{salinity}$; Chen *et al.* [1986]), ^{234}Th is the measured activity of total ^{234}Th , λ is the decay constant for ^{234}Th ($= 0.0288 \text{ day}^{-1}$), P is the net removal flux of ^{234}Th on particles, and V is the sum of advective and diffusive ^{234}Th fluxes.

The particle flux P is positive for a net downward flux or negative if there is an upward flux. Since there are no significant aeolian ^{234}Th sources, ^{234}Th activities in surface waters are generally at secular equilibrium with ^{238}U if particle export is limited, or $^{234}\text{Th} < {}^{238}\text{U}$ if export is significant. For intermediate depths, $^{234}\text{Th} > {}^{238}\text{U}$ can be found, if sinking particles carrying ^{234}Th remineralize, and form an additional ^{234}Th source at depth [Buesseler *et al.*, 1992a]. Most often the ^{234}Th remineralization rate is small relative to the inventory at a given depth, therefore ^{234}Th activities in excess of ^{238}U are not frequently observed.

Using the simple activity balance in (4), ^{234}Th particle fluxes P can be calculated from a knowledge of the other terms in the equation, assuming a constant particle flux between measurements. The reliability of this approach therefore hinges upon our ability to quantify each of the source and sink terms. In most situations, the particle flux P is driven by the relatively small difference between ^{238}U and ^{234}Th activities, as the other terms in (4) contribute only slightly to the overall activity balance. As such, the precision and accuracy of the ^{234}Th determination is critical.

Steady state models. The first trap calibration analysis is to simply compare the measured trap fluxes with the fluxes calculated from (4), assuming that temporal changes are insignificant and that advective and diffusive fluxes are small ($\partial^{234}\text{Th}/\partial t = 0$ and $V = 0$ in equation (4)). The ^{234}Th particle flux thus calculated at each point ranges from -300 to +237 dpm/m²/d (Table 2; negative fluxes represent net import of ^{234}Th into the upper 0-96-m layer, and positive fluxes export out of this layer). This calculation is similar to all previously published studies where a single profile of ^{234}Th is compared to the measured trap flux (such as *Coale and Bruland* [1985, 1987]). Using this first-order flux calculation, we find no overlap between any of the calculated and measured fluxes, and in only 4 of the 26 cases (15%) is the calculated flux within a factor of two of the measured value. Using the mean and standard deviation of all of the ^{234}Th data (2.53 ± 0.05), we calculate a particulate ^{234}Th export flux of -27 ± 138 dpm/m²/d. This flux overlaps with zero and is significantly lower than any of the four measured trap fluxes (Figure 3).

We have estimated above that the particle source region has a length scale of the order of <1-10 km. The analysis above used all of the data, thereby assuming the larger length scale. If one assumes the lower limit is correct, then one should compare the trap fluxes to the ^{234}Th activity directly over the traps. Using the mean ^{234}Th activity over the traps ($n = 11$ @PITS; Table 2), we calculate a ^{234}Th particle flux of $+17 \pm 141$ dpm/m²/d. This is still significantly lower than the measured trap fluxes. Since the mean ^{234}Th activity from the 6-km grid points is slightly higher, the mean flux calculated using only the 6-km grid points (-75 ± 100 dpm/m²/d, $n = 11$) is even further from the measured flux.

As stated previously, we feel that the most appropriate model for comparing the trap flux and the surface water ^{234}Th budget is one where we consider the trap as relatively "fixed," with numerous particle source waters passing over the trap each day. In this Lagrangian approach, the motion of each parcel of fluid and particles is determined by the mesoscale eddy field above the trap. As the parcel passes over the trap, any sinking particles originating from this source region should be caught in the trap, and the flux at that moment would be quantified by the measured ^{234}Th / ^{238}U disequilibria. The difference with the previous calculation is that the data are treated in a stepwise fashion, and each of the calculated fluxes is assumed to represent the steady state trap flux only for a short time interval. For example, each of the five pairs of PITS water data are used to define four time intervals over which the steady state ^{234}Th model is used to calculate the flux for a given time interval. In this manner, a flux of 87 dpm/m² is calculated for the period between 1800 LT May 4 and 1430 LT May 5, 9 dpm/m² between this last point and 0755 LT May 6 -129 dpm/m²

through 1400 LT May 7, and -59 dpm/m² until the end (1555 LT May 8; data taken from Table 2). Adjusting for the time intervals and assuming that the traps can only measure positive flux (i.e., sinking particles), one would calculate an expected trap flux of 25 dpm/m²/d ((87 + 9)dpm/m²/3.9 days) for the duration of the experiment. Again, this is much lower than the measured trap flux of 290 dpm/m²/d. Using the data from the 6-km grid points would produce an even larger difference between the measured and calculated flux.

Non-steady state model. In order to estimate $\partial^{234}\text{Th}/\partial t$, one must measure the time-varying ^{234}Th activity in a single parcel of water. In most cases, since the particle source region is small and surface currents are large, the water one samples each day originates beyond the immediate particle source waters. We therefore must assume that any temporal trends in bulk water activity are common to a larger spatial region. Prior work with ^{234}Th has shown that the assumption of steady state for ^{234}Th is generally appropriate, except during periods of intense change in scavenging intensity, such as the onset of the spring bloom in the NE Atlantic [*Buesseler et al.*, 1992a]. If temporal changes are significant, one can solve (4) without relying on the assumption of steady state. In this case the exact solution becomes (including a non-steady state term, $\partial^{234}\text{Th}/\partial t$, but still ignoring V):

$$^{234}\text{Th}_2 = ^{238}\text{U}(1 - e^{-\lambda t_2}) + ^{234}\text{Th}_1 e^{-\lambda t_2} - \left(\frac{P}{\lambda}\right)(1 - e^{-\lambda t_2}) \quad (5)$$

where $^{234}\text{Th}_1$ and $^{234}\text{Th}_2$ are the activities of ^{234}Th at t_1 and t_2 , respectively (Appendix A of *Buesseler et al.* [1992a]). The particle flux P can be determined using time series ^{234}Th data and a curve fitting routine which minimizes the difference between the model and the data, leaving both $^{234}\text{Th}_1$ and the flux P as unknowns. If we use our data and this non-steady state model, we calculate a ^{234}Th flux of -1500 ± 1000 dpm/m²/day. As stated above, we do not see any statistically significant temporal trends in our data, hence the uncertainty on the fit to the non-steady state model is quite large. The solution predicts an increasingly negative flux, relative to the steady state model, which is consistent with the slight but not statistically significant increase in ^{234}Th activity with time (Figure 2).

Horizontal advective/diffusive fluxes. The thorium scavenging model has an advection-diffusion term V that accounts for the addition or loss of ^{234}Th by fluxes from adjacent waters. In order to calculate the horizontal component of these fluxes, we need an estimate of the activity gradients within the data set, and we must assume that the horizontal gradients are actively maintained by vertical fluxes within the study site. In other words, there must be a concentration difference between the water entering our study site and the water exiting the site in order to support a convergence of horizontal fluxes. As mentioned above, within our 0.05 dpm/kg activity error, there are no significant gradients in ^{234}Th between the samples at the PITS and those further removed at 6 or 10 km. Thus, to a first approximation, the horizontal flux term is zero in (4).

In order to evaluate this horizontal flux term further, we first attempt to determine the relative magnitude of advective versus diffusive fluxes for the ^{234}Th balance. To do this, we evaluate the dimensionless parameter $U_h \ell / K_h$, also known as a Peclet number P_e which scales the importance of advection versus eddy

diffusion. For this site we will use 100 km (10^5 m) as the length scale ℓ of the expected horizontal concentration gradients, a measured surface current velocity of 0.2 m/s U_h , and the nearest neighbor diffusivity K_h of 1 m²/s calculated from the surface drogues (see Particle Source Region). Using these values, $P_e = 2 \times 10^4$, which indicates that advective fluxes dominate over diffusive ones. This value of P_e is so large that even if any of the terms were off by three orders of magnitude, this conclusion would still hold. As such, we will focus our attention on our ability to constrain the advective fluxes in the ²³⁴Th balance. In this case, V_{horz} would reduce to $U_h \partial \text{Th} / \partial x$. Since we can only measure ²³⁴Th with a precision of 0.05 dpm/kg (50 dpm/m³) and the maximum horizontal distance over which this was measured in our study was 20 km, all we can say is that $\partial \text{Th} / \partial x < 2.5 \times 10^{-3}$ dpm/m⁴. Given the observed surface current of 0.2 m/s (1.7×10^4 m/d), this would imply a V_{horz} of < 42.5 dpm/m³/d. Unfortunately, this advection term is not well constrained, relative to the production and decay terms for ²³⁴Th in (4) which in these same units are of the order of 70 dpm/m³/d. If the deficit of ²³⁴Th was larger, then the magnitude of V may be negligible relative to the ²³⁴Th production and decay terms, but this must be shown in each study.

Typically, no attempt is made to measure V , as this would require a complete knowledge of tracer activity and water velocities at every depth and time over the trap, both on the spatial scales of the immediate particle source region (i.e., 1-10 km) and over larger scales to tightly constrain the uncertainty on $\partial \text{Th} / \partial x$. This is clearly beyond the scope of our study. In oceanography, simple one-dimensional models are frequently used to interpret vertical profile of any chemical species in the oceans; and this is generally accepted. Our inability to estimate the exact magnitude of horizontal advective fluxes for any radiotracer, or for that matter, heat, POC, or nutrient stocks, will ultimately limit the usefulness of any mass balance approach and remains the largest uncertainty in our ²³⁴Th model and perhaps in the validation of fluxes of any type.

Vertical advective/diffusive fluxes. In some published ²³⁴Th profiles there is an excess of ²³⁴Th over ²³⁸U below the euphotic zone due to remineralization. In fact, this excess must occur, on average, in any environment with strong surface scavenging, but it is hard to measure because of the large depth range over which it is averaged. A subsurface excess in our area could result in a vertical flux by diapycnal mixing that would balance the downward flux on particles. This subsurface maximum would have to be introduced horizontally as there is no scavenging from above. Thus with this scenario, we must hypothesize the presence of a high scavenging environment somewhere other than our sampling area that results in a subsurface excess of ²³⁴Th from remineralization. This subsurface remineralization must then be moved horizontally to the water below our site. Unfortunately, we did not measure the activity of the water below the traps and cannot test this hypothesis directly. However, we can use our existing data to place bounds on such a process and to evaluate its likelihood.

First, we can calculate the size of the ²³⁴Th excess inventory that would be required to balance the sediment trap flux of 300 dpm/m²/day (0.0035 dpm/m²/s). From the required flux and an assumed diapycnal (i.e., vertical) eddy diffusivity of 0.1×10^{-4} m²/s we estimate that a gradient of 0.35 dpm/kg/m is required at a depth of 96 m, that is, a ²³⁴Th excess activity of

0.7 dpm/kg only 2 m below the trap. Excess ²³⁴Th activities of 0.2-0.3 dpm/kg are rare, even under areas of high scavenging [Coale and Bruland, 1985; Buesseler et al., 1992a]. If the eddy diffusivity was an order of magnitude larger, the gradient would be tenfold lower, and a ²³⁴Th excess of 0.5 dpm/kg would be exceeded 14 m below the trap. Excess ²³⁴Th activities of 0.5-0.7 dpm/kg are unlikely at this or any other site.

Possible Trap Biases

From our data and within the limits of our model it appears that the sediment trap overcollected particulate matter in this instance. This does not mean that traps overcollect under all conditions and for all particle types or that future tests on the remaining assumptions in our ²³⁴Th models are not warranted, such as further constraining advective and diffusive terms. If we accept that this particular trap did overcollect, we can move on to an evaluation of the possible causes of that oversampling. We suggest that the previously described hydrodynamic effects on collection [Gardner 1980; Butman et al., 1986] and the inclusion of swimmers in the trap material [Knauer et al., 1984; Michaels et al., 1990] are two possible sources of error in trap collections.

Hydrodynamics. The flow regime around and within a trap is known to affect the collection of sinking particles [Gardner, 1980; Butman et al., 1986; Baker et al., 1988]. For VERTEX-style traps it is generally believed that flows of less than 15 cm/s are unlikely to affect the collection of sinking particles [e.g., Knauer and Asper 1989]; however, some studies [White, 1990; Gust et al., 1992] find that flow past a sediment trap affects collection efficiencies even at lower velocities. In this study the mean flow at the mouth of the sediment trap was 8.2 cm/s, which is on the low end of approach velocities typically found for BATS sediment trap deployments (6-24 cm/s; Johnson et al., 1991; also G. Gust, unpublished data, 1994). The flow on this array may have been reduced because of the concentration of drag elements at the trap depth. Most of the cross-sectional area on any trap array is due to the line (for a half inch line there is 1.27 m² of area for every 100 m of line). For this array there was no line below the trap depth. We had three packages around 95 m and little subsurface or surface flotation. This concentration of the cross-sectional area and drag near the depth of the traps probably contributed to the lower velocity. Traditional MultiPIT arrays extend to 400 m (BATS array), 500 m (Hawaii Ocean Time-Series), or even 2000 m (VERTEX array, JGOFS North Atlantic Bloom Experiment).

The internal velocity of water measured by the HDS package on the downstream side of the trap tube just below the baffle was 1.16 cm/s or 14% of the measured approach velocity at the trap mouth (Figure 4). In previous deployments, the ratio of internal flow to approach velocity ranged from 10-50%. From this internal velocity and given that the inflow circulation cells cover ~40% of the trap area (G. Gust, unpublished data, 1994) we can calculate that the upper trap flushing rate was 18 cm³/s. This implies that over 6,000 L of seawater and particles flushed through a single cylinder during the 4-day deployment. In this study, each trap collected an average of 400 µg of carbon during the deployment. With measured ambient carbon concentrations of 20-30 µg/L, this represents 0.2-0.3% of the total suspended POC in the water (i.e., 6000 L) that passed through the trap. In many of the other BATS deployments the internal flows have

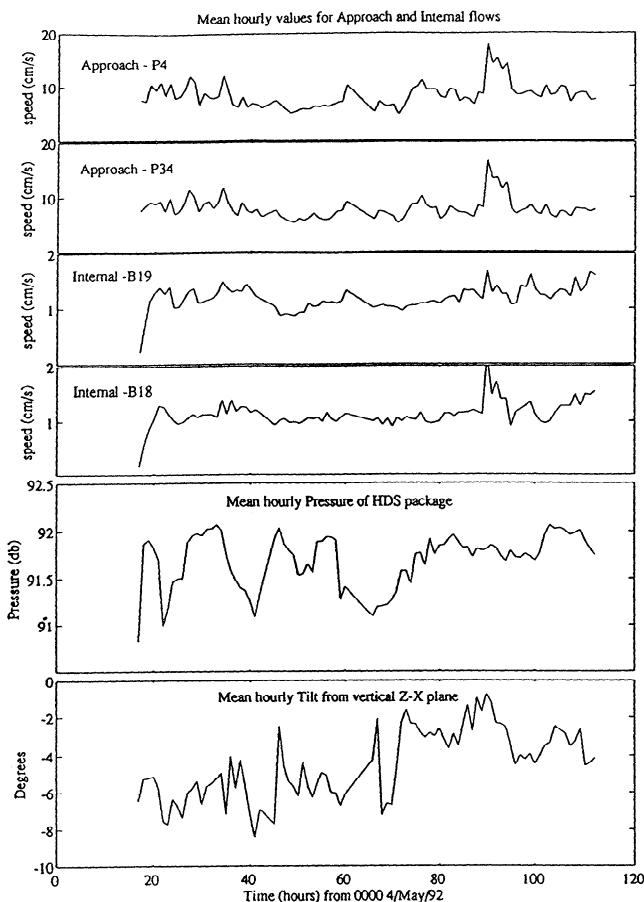


Figure 4. Flow, pressure, and tilt results from the sediment trap calibration experiment in May 1992. All values are hourly means. The upper two panels are the results for the approach velocity sensors near the mouth of the traps. The middle two panels are for two sensors placed just below the baffles inside the traps. Note the coherence of the flow events throughout the deployment. The bottom two panels are for the pressure and one of the tilt sensors located inside the HDS package, mounted on the trap frame.

been as much as 10-fold higher. *Butman et al.* [1986] suggest that sheer stress might enhance aggregation or disaggregation of particles within the trap depending upon the trap Reynolds number and the specific particle mixture. In general, sheer forces are thought to enhance coagulation processes and thus would increase particle fall velocities [*McCave*, 1984; *Farley*, 1990; *Jackson*, 1990; *Hill*, 1992]. With the large volume of water passing through a trap and the very small amount of carbon that is collected, even a small amount of particle aggregation induced by sheer in the trap would be sufficient to make a significant positive bias in the total sediment trap collection (G. Gust, unpublished data, 1994). As such, the traps would be acting analogous to a very inefficient in situ filter, removing a small fraction of the suspended particulate pool.

Gardner [1985] tested the effect of trap tilt on collection and found that cylindrical traps tended to overcollect when tilted compared to the upright cylinder. This overcollection was ~25% for tilts of 5° like those observed in this study (Figure 4). This

predicted bias is in the correct direction as the observed overcollection, however, our measured overcollection appears to be greater than 25%.

Swimmers. Zooplankton are a common component of sediment trap samples, particularly those deployed near the euphotic zone. In some studies, sediment traps have been placed over 100 m below the base of the euphotic zone because swimmer contamination is so great, even though this results in difficulty in later determination of the export fluxes [*Martin et al.*, 1993]. Swimmers may also release detrital material into a trap that will be identical to the sinking detritus that we assume a trap collects naturally [*Michaels et al.*, 1990]. Swimmers have a large effect on the estimates of carbon fluxes but are likely to be less of a problem for ^{234}Th . The picked swimmers in this study have a high C:Th ratio ($= 7 \mu\text{mol/dpm}$; Tables 3 & 4). Thus even if half of the remaining carbon was due to swimmers, it would only be a 10% error in the thorium. Swimmer products and detritus may have lower C:Th ratios, but there are no data available to address this issue. However, because swimmers do result in an overcollection of material, or over estimate of fluxes, swimmers or their products are a possible mechanism to explain our results. Swimmer removal from these traps uses the same intensive visual techniques developed by Knauer and coworkers. Many other research groups use more generalized techniques like screening or a less intensive visual removal of swimmers which have more uncertain results. Clearly, if the excess of thorium over the predicted flux in this study is due to swimmers or swimmer products which we did not remove manually, then this is a generic accuracy problem that is likely much worse with the total carbon pools.

If each sediment trap flushed 6 m^3 during the deployment, the zooplankton may be carried into the trap by the flow, not finding it with their own motility. The term "swimmers" might be a misnomer in this case (more aptly, these zooplankton are "surfers"). Once in the trap flow cell, natural escape responses like a downward swimming motion would accelerate their collection in the trap. Defecation on disturbance or the loss of a larvacean's house when disturbed may add sinking particles to the flow cell that are not naturally a part of the ambient sinking particle pools.

Implications

This trap calibration was done in concert with the time-series program at BATS. At this site there are now four years of intensive monthly measurements of hydrography, particle stocks, primary production, and sediment trap-sensed fluxes. These data provide a further context for interpreting the results and implications of this study. For this single deployment we predict a zero ^{234}Th flux on particles. It is an open question whether this translates into a zero carbon flux. There are no records of a zero flux at the BATS site or for that matter in any trap deployment ever published. Logically, if a trap came up empty, one might assume that it had lost its contents, rather than that nothing was sinking. At the BATS and other oceanic sites around the world, the range of fluxes at 150 m is quite narrow. The lowest flux at BATS is $17.7 \text{ mg C/m}^2/\text{d}$, and the highest is $55 \text{ mg C/m}^2/\text{d}$. In the VERTEX seasonal study, particulate carbon fluxes at 150 m ranged from 13 to $24 \text{ mg C/m}^2/\text{d}$, although they were later multiplied by 2.23 to compensate for an

assumed dissolution in the trap [Knauer et al., 1990]. For the earlier VERTEX deployments, some of which occurred in more productive waters, fluxes near 150 m ranged from 22 to 70 mg C/m²/d with the exception of a much higher flux measured at the VERTEX 5c station in the upwelling areas near the California Coast [Martin et al., 1987]. The constancy of these fluxes has been one of the cited reasons to indicate that the fluxes are accurate [Knauer and Asper, 1989].

At the BATS site, we now have over 50 sediment trap deployments of 3-4 days duration. These were collected on a monthly basis using the standard VERTEX techniques [Lohrenz et al., 1992]. The sediment trap data show seasonal patterns that appear to be coincident with the seasonal patterns in production. The mean annual nitrogen flux for the four-year period is 0.1 moles N/m²/yr. This trap flux is only 14-25% of the long-term average new production estimated by a variety of techniques that average over long time and large space scales [Jenkins and Goldman, 1985; Jenkins, 1980]. Although the BATS deployment is only 3-4 days out of each month, with the large number of deployments it is statistically highly improbable that the difference between the Jenkins and Goldman [1985] new production of 0.4-0.7 moles N/m²/yr and the BATS trap flux is because the BATS traps were never deployed during the high flux events.

Even on shorter timescales there are data to indicate that new production each year must be higher than the annual sediment trap nitrogen flux. Each spring the mixed layer deepens to between 150 and 300 m with mixed layer temperatures of 18-19°C. This deep mixing brings subsurface nitrate into the euphotic zone, and shortly after stratification, the nitrate in the upper 100 m is used to support new phytoplankton production. The mixed layer concentrations of nitrate can be inferred from the density of the water and the tight correlation between nitrate and density in the main thermocline. These concentrations vary between 0.2 and 4.05 mol/kg. The depletion of this nitrate stock in the upper 100 m accounts for a new production between 0.02 and 0.4 moles N/m². This must be an underestimate of the total spring new production because of continued mixing of nitrate into the euphotic zone as it is depleted near the surface.

It also seems likely that the sediment trap-estimated particle flux must be lower than the total new production from previous thorium data. There are a number of observations of net thorium deficits of up to 20% [Moran and Buesseler, 1992; M. Bacon, personal communication, 1994]. These activities predict a flux of 1400-2200 dpm/m²/d. If we convert this to carbon using the carbon:thorium ratio seen in this study (= 7 µmol/dpm; Table 4), we would predict a carbon flux of 121-181 mg C/m²/d. This is 2-3 times as high as the largest measured carbon flux of 55 mg C/m²/d and three times as high as the next largest flux.

From these studies we conclude that the BATS annual sediment trap fluxes are lower than the new production which occurs in the short spring bloom period and are 4-7 times lower than the annual new production. Some of this difference may be due to other processes that transport organic matter from the surface to the deep sea. Higher concentrations of dissolved organic nitrogen near the surface might be physically mixed below the surface and partially compensate for the upward mixing of nitrate. Vertically migrating zooplankton may consume material at the surface and excrete ammonia at depth, resulting in a net downward transfer [Longhurst and Harrison, 1988].

In summary, from this study and the existing long-term record of trap fluxes at BATS, the evidence suggests that periods of either overcollection (during low flux periods) or undercollection (during high flux periods) are possible. Since the baseline sediment trap flux is so consistent, we hypothesize that there is a continuous collection of nonsinking material or an overcollection of slowly sinking particles. This may arise from the aggregation caused by shear of the circulation cell in the mouth of the trap, or perhaps by the routine collection of swimmers and swimmer products throughout the year [Michaels et al., 1990]. Thus in low flux periods the traps probably overcollect. The traps also seem to underestimate C flux, or new production during the periods of high fluxes, and also underestimate total annual flux. However, the timing of the flux events is nearly always correct, and the traps do seem to reproduce the seasonal cycle correctly (this may be tautological as our current perceptions of the seasonal cycle of export are based on trap data). We therefore hypothesize that the sediment traps at the BATS site yield a damped seasonal signal.

The major implication of the damped seasonal signal of flux is that the particle flux does not increase by the same relative amount as the primary production. Primary production increases over tenfold between January and March. Trap fluxes never increase by more than threefold. This difference in amplitude of the seasonal cycles results in the reported inverse relationship between trap estimates of new production and the total production [Knauer et al., 1990; Lohrenz et al., 1992]. This inverse relationship has always been a bit troublesome as the majority of the nitrate input must occur during the periods of deep mixing. If the trap signal is modulated by hydrodynamics and seasonal variability in the problems with swimmers, the inverse relationship may be more of a sampling problem than a process in nature.

Conclusions

A central goal of any trap calibration experiment is to compare the measured trap flux with some other independent measure of particle flux. In this study we find that the traps overcollected ²³⁴Th at this time and place. We support this conclusion by measuring ²³⁴Th in the watercolumn at 27 points in space and time and on four sets of traps on two floating arrays during a four-day period. Our calibration does not appear to be affected by swimmer-related transport of ²³⁴Th, non-steady state conditions, spatial variations in ²³⁴Th, or horizontal or vertical advective and diffusive fluxes, but this need not apply to other studies or sites. The future application of ²³⁴Th as a calibrator of upper ocean sediment traps will require careful attention to the accuracy and precision of the ²³⁴Th activity determinations and further development of the ²³⁴Th model, particularly as it relates to constraining advective transport of ²³⁴Th. Also, continued studies of the relationship between the flux of ²³⁴Th and organic C will be needed to determine if the ²³⁴Th calibration can be applied to other components of the sinking particulate pool.

We would argue that the degree of over or undercollection for traps will be a function of particle type (primarily sinking speed) and local hydrodynamics. Despite this concern, trap data may qualitatively suggest a pattern of export which seems reasonable, that is, highest during bloom conditions and lowest at more oligotrophic sites, and as a function of depth. Ultimately, the absolute degree of certainty one needs to answer

a given oceanographic question will determine whether or not the measured flux obtained by traps is useful. From ^{234}Th , most shallow traps would appear to be calibrated within a factor of 2-3 in both positive and negative directions [Buesseler, 1991]. Until we understand more clearly the relationship between the collected flux, particle type, and trap hydrodynamics in the field, we would suggest that ^{234}Th calibrations be conducted as part of each trap deployment. Traps are clearly an important tool, and the property we hope to measure with traps, the vertical flux of particles, is important for many questions in oceanography. As we enter into an era of satellite oceanography and basin-wide estimates of surface water productivity and carbon uptake, it will be important to develop accurate tools for the estimation of particle export to understand and quantify the fate of carbon and associated elements in the oceans.

Acknowledgments. This work would not have been possible without the use of the Hydrodynamic Sensing package provided by Giselher Gust (T.U. Hamburg-Harburg). For technical support we would like to thank Rod Johnson, Steve Seibel, Steve Jayne, and Kjell Gundersen (all at BBSR) and Mary Hartman (WHOI). We were generously assisted in our statistical analyses by Andrew Solow (WHOI) and for ^{238}U analyses by R. L. Edwards and J. Hoff (U. of Minnesota). Reviews by R. Anderson and W. Moore as well as comments from M. Bacon, W. Jenkins, G. Gust, and K. Stolzenbach greatly improved this manuscript. Secretarial assistance of Sheila Clifford is also appreciated. Support for this work was provided by NSF (OCE-9123888), (OCE-9016990), (OCE-9201186), and (OCE-8801089). This is contribution 8614 from WHOI and 1351 from BBSR.

References

- Bacon, M. P., C. A. Huh, A. P. Fleer, and W. G. Deuser, Seasonality in the flux of natural radionuclides and plutonium in the deep Sargasso Sea, *Deep Sea Res., Part A*, 32, 273-286, 1985.
- Baker, E. T., H. B. Milburn, and D. A. Tennant, Field assessment of sediment trap efficiency under varying flow conditions, *J. Mar. Res.*, 46, 573-592, 1988.
- Blackwelder, R. F., Hot-wire and hot-file anemometers, in *Methods of Experimental Physics: Fluid Dynamics*, edited by R. J. Emrich, pp. 259-314, Academic, San Diego, Calif., 1981.
- Buat-Ménard, P., J. Davies, E. Remoudaki, J. C. Miquel, G. Bergametti, C. E. Lambert, U. Ezat, C. Quetel, J. La Rosa, and S. W. Fowler, Non-steady-state biological removal of atmospheric particles from Mediterranean surface waters, *Nature*, 340, 131-134, 1989.
- Buesseler, K. O., Do upper-ocean sediment traps provide an accurate record of particle flux?, *Nature*, 353, 420-423, 1991.
- Buesseler, K. O., H. D. Livingston, S. Honjo, B. J. Hay, T. Konuk, and S. Kempe, Scavenging and particle deposition in the southwestern Black Sea - Evidence from Chernobyl radiotracers, *Deep Sea Res., Part A*, 37, 413-430, 1990.
- Buesseler, K. O., M. P. Bacon, J. K. Cochran, and H. D. Livingston, Carbon and nitrogen export during the JGOFS North Atlantic bloom experiment estimated from ^{234}Th : ^{238}U disequilibria, *Deep Sea Res., Part A*, 39, 1115-1137, 1992a.
- Buesseler, K. O., J. K. Cochran, M. P. Bacon, H. D. Livingston, S. A. Casso, D. Hirschberg, M. C. Hartman, and A. P. Fleer, Determination of thorium isotopes in seawater by non-destructive and radiochemical procedures, *Deep Sea Res., Part A*, 39, 1103-1114, 1992b.
- Butman, C. A., W. D. Grant, and K. D. Stolzenbach, Predictions of sediment trap biases in turbulent flows: A theoretical analysis based on observations from the literature, *J. Mar. Res.*, 44, 601-644, 1986.
- Chen, J. H., R. L. Edwards, and G. J. Wasserburg, ^{238}U , ^{234}U and ^{232}Th in seawater, *EPSL*, 80, 241-251, 1986.
- Coale, K., and K. W. Bruland, ^{234}Th : ^{238}U disequilibria within the California Current, *Limnol. Oceanogr.*, 30, 22-33, 1985.
- Coale, K., and K. W. Bruland, Oceanic stratified euphotic zone as elucidated by ^{234}Th : ^{238}U disequilibria, *Limnol. Oceanogr.*, 32, 189-200, 1987.
- Deuser, W. G., Seasonal and interannual variations in deep-water particle fluxes in the Sargasso Sea and their relation to surface hydrography, *Deep Sea Res., Part A*, 33, 225-246, 1986.
- Deuser, W. G., F. E. Muller-Karger, and C. Hemleben, Temporal variations of particle fluxes in the deep subtropical and tropical North Atlantic: Eulerian versus Lagrangian effects, *J. Geophys. Res.*, 93, 6857-6862, 1988.
- Eppley, R. W., and B. J. Peterson, Particulate organic matter flux and planktonic new production in the deep ocean, *Nature*, 282, 677-680, 1979.
- Eppley, R. W., E. H. Renger, and P. R. Betzer, The residence time of particulate organic carbon in the surface layer of the ocean, *Deep Sea Res., Part A*, 30, 311-323, 1983.
- Farley, K. J., Predicting organic accumulation in sediments near marine outfalls, *J. Environ. Eng. N. Y.*, 116, 144-165, 1990.
- Fleer, A. P., Updated determination of particulate and dissolved thorium-234, in *Marine Particles: Analysis and Characterization*, *Geophys. Monogr. Ser.*, vol. 63, edited by D. C. Hurd and D. W. Spencer, pp. 227-228, AGU, Washington, D.C., 1991.
- Fowler, S. W., and G. A. Knauer, Role of large particles in the transport of elements and organic compounds through the oceanic water column, *Prog. Oceanogr.*, 16, 147-194, 1986.
- Gardner, W. D., Sediment trap dynamics and calibration: A laboratory evaluation, *J. Mar. Res.*, 38, 17-39, 1980.
- Gardner, W. D., The effect of tilt on sediment trap efficiency, *Deep Sea Res., Part A*, 32, 349-361, 1985.
- Gust, G., R. H. Byrne, R. E. Bernstein, P. R. Betzer, and W. Bowles, Particle fluxes and moving fluids: Experience of synchronous trap collections in the Sargasso Sea, *Deep Sea Res., Part A*, 39, 1071-1083, 1992.
- Hill, P. S., Reconciling aggregation theory with observed vertical fluxes following phytoplankton blooms, *J. Geophys. Res.*, 97, 2295-2308, 1992.
- Hitchcock, G. L., D. B. Olson, G. A. Knauer, A. A. P. Pszenny, and J. N. Galloway, Horizontal diffusion and new production in the Sargasso Sea, *Global Biogeochem. Cycles*, 4, 253-265, 1990.
- Jackson, G. A., A model of the formation of marine algal flocs by physical coagulation processes, *Deep Sea Res., Part A*, 37, 1197-1211, 1990.
- Jenkins, W. J., Nitrate flux into the euphotic zone near Bermuda, *Nature*, 331, 521-523, 1988.
- Jenkins, W. J., and J. C. Goldman, Seasonal oxygen cycling and primary production in the Sargasso Sea, *J. Mar. Res.*, 43, 465-491, 1985.
- Johnson, R., G. Gust, W. Bowles, A. Michaels, and A. Knap, Flows around surface-tethered sediment traps (multitraps) at the U.S. JGOFS Bermuda Atlantic time-series station, paper presented at The Oceanography Society Second Scientific Meeting, Oceanogr. Soc., St. Petersburg, FL, 1991.
- Karl, D. M., B. D. Tilbrook, and G. Tien, Seasonal coupling of organic matter production and particle flux in the western Bransfield Strait, Antarctica, *Deep Sea Res., Part A*, 38, 1097-1126, 1991.
- Knap, A. H., et al., Bermuda Atlantic time-series study - BATS Method Manual, version 3, 108 pp., U.S. JGOFS Plann. and Coord. Office, Woods Hole Oceanogr. Inst., Woods Hole, Mass., 1993.
- Knauer, G. A., and V. Asper, Sediment trap technology and sampling, *U.S. GOFs Plann. Rep. 10*, 94 pp., U.S. GOFs Plann. Office, Woods Hole, Mass., 1989.

- Knauer, G. A., J. H. Martin, and K. W. Bruland, Fluxes of particulate carbon, nitrogen, and phosphorus in the upper water column of the northeast Pacific, *Deep Sea Res., Part A*, 26, 97-108, 1979.
- Knauer, G. A., D. M. Karl, J. H. Martin, and C. N. Hunter, In situ effects of selected preservatives on total carbon, nitrogen and metals collected in sediment traps, *J. Mar. Res.*, 42, 445-462, 1984.
- Knauer, G. A., D. G. Redalje, W. G. Harrison, and D. M. Karl, New production at the VERTEX time-series site, *Deep Sea Res., Part A*, 37, 1121-1134, 1990.
- Livingston, H. D., and R. F. Anderson, Large particle transport of plutonium and other fallout radionuclides to the deep ocean, *Nature*, 303, 228-231, 1983.
- Lohrenz, S. E., G. A. Knauer, V. L. Asper, M. Tuel, A. F. Michaels, and A. H. Knap, Seasonal and interannual variability in primary production and particle flux in the northwestern Sargasso Sea: U.S. JGOFS Bermuda Atlantic Time Series, *Deep Sea Res., Part A*, 39, 1373-1391, 1992.
- Longhurst, A. R., and W. G. Harrison, Vertical nitrogen flux from the oceanic photic zone by diel migrant zooplankton and nekton, *Deep Sea Res., Part A*, 35, 881-889, 1988.
- Martin, J. H., and G. A. Knauer, VERTEX: Manganese transport through oxygen minima, *Earth Planet. Sci. Lett.*, 67, 35-47, 1984.
- Martin, J. H., G. A. Knauer, D. M. Karl, and W. W. Broenkow, VERTEX: Carbon cycling in the northeast Pacific, *Deep Sea Res., Part A*, 34, 267-285, 1987.
- Martin, J. H., S. E. Fitzwater, R. M. Gordon, C. N. Hunter, and S. J. Tanner, Iron, primary production and carbon-nitrogen flux studies during the JGOFS North Atlantic Bloom Experiment, *Deep Sea Res., Part A*, 40, 115-134, 1993.
- McCave, I. N., Size spectra and aggregation of suspended particles in the deep ocean, *Deep Sea Res., Part A*, 31, 329-352, 1984.
- Michaels, A. F., M. W. Silver, M. M. Gowing, and G. A. Knauer, Cryptic zooplankton "swimmers" in upper ocean sediment traps, *Deep Sea Res., Part A*, 37, 1285-1296, 1990.
- Michaels, A. F., et al., Seasonal patterns of ocean biogeochemistry at the U.S. JGOFS Bermuda Atlantic time-series study site, *Deep Sea Res., Part A*, in press, 1994.
- Moore, W. S., K. W. Bruland, and J. Michel, Fluxes of uranium and thorium series isotopes in the Santa Barbara Basin, *Earth Planet. Sci. Lett.*, 53, 391-399, 1981.
- Moran, S. B., and K. O. Buesseler, Short residence time of colloids in the upper ocean off Bermuda, *Nature*, 359, 221-223, 1992.
- Noshkin, V. E., and E. DeAgazio, Low background beta detector for solid sample assay, *Nuclear Instrum. Methods*, 39, 265-270, 1966.
- Okubo, A., Oceanic diffusion diagrams, *Deep Sea Res., Part A*, 18, 789-802, 1971.
- Osterberg C. A., G. Carey, Jr., and H. Curl, Jr., Acceleration of sinking rates of radionuclides in the ocean, *Nature*, 200, 1276-1277, 1963.
- Siegel, D. A., T. C. Granata, A. F. Michaels, and T. D. Dickey, Mesoscale eddy diffusion, particle sinking, and the interpretation of sediment trap data, *J. Geophys. Res.*, 95, 5305-5311, 1990.
- Tsunogai, S., K. Taguchi, and K. Harada, Seasonal variation in the difference between observed and calculated particulate fluxes of Th-234 in Funka Bay, Japan. *J. Oceanogr. Soc. Jpn.*, 42, 91-98, 1986.
- Wei, C-L., and J. W. Murray, Temporal variations of ^{234}Th activity in the water column of Dabob Bay: Particle scavenging, *Limnol. Oceanogr.*, 37, 296-314, 1992.
- White, J., The use of sediment traps in high-energy environments, *Mar. Geophys. Res.*, 12, 145-152, 1990.
-
- K. O. Buesseler, Department of Marine Chemistry and Geochemistry, Woods Hole Oceanographic Institution, Woods Hole, MA 02543. (e-mail: kbuesseler@whoi.edu)
- A. H. Knap and A. F. Michaels, Bermuda Biological Station for Research, Incorporated, 17 Biological Ln., Ferry Reach, GE01 Bermuda.
- D. A. Siegel, Center for Remote Sensing and Environmental Optics and Department of Geography, University of California, 3611 Ellison Hall, Santa Barbara, CA 93106.

(Received August 16, 1993; revised January 4, 1994; accepted January 21, 1994.)